

Cirrus cloud thinning using a more physically-based ice microphysics scheme in the ECHAM-HAM GCM (acp-2021-685)

Colin Tully, David Neubauer, Nadja Omanovic, and Ulrike Lohmann

Referee #2 Author Response

Thank you for taking the time to review our manuscript and for providing useful comments on improving this study. We have quoted each of your comments below with our response.

1. **Comment:** Line 197-199: If you are using the Karcher et al 2006 method to represent ice nucleation, which includes water vapor consumption, why is there a need to add a downdraft to update the water vapor consumption? More explanation is needed here.
 - a. **Response:** The cirrus model works such that changes to the ice saturation ratio (S_i) only occur by the updraft. Therefore, we need some way of altering this variable to account for the effect of water vapor consumption during ice formation events or onto pre-existing ice crystals in a single cirrus model timestep. We calculate an updated updraft velocity every cirrus model timestep, with the deposited water vapor accounted for by the fictitious downdraft. Although the amount of water vapor consumption in one cirrus timestep may not completely deplete ice supersaturation (and therefore shut off further ice formation/growth), the consumption will alter the way the updraft evolves and therefore how the S_i evolves in subsequent cirrus model timesteps. We altered the text to make this clearer for readers.
 - b. **Changes in the text at lines 190-193, and 198-202:**

“... The scheme uses a sub-stepping approach to simulate the temporal evolution of ice saturation during the formation-stage of a cirrus cloud. This is achieved by calculating the balance between the adiabatic cooling of rising air, with the associated saturation increase, and the diffusional growth of ice particles that consume the available water vapor. ...”

As the magnitude of the ice saturation ratio is determined only by the vertical velocity, a fictitious downdraft is introduced at the end of each timestep of the cirrus scheme to quantify the effect of water vapor consumption during new ice formation events or onto pre-existing ice particles (Kuebbeler et al., 2014). The updated vertical velocity therefore determines the evolution of the ice saturation ratio in sub-sequent sub-timesteps. ...”

2. **Comment:** Line 219-220: What is the time step in the cirrus scheme that is referred to here? Is it the 7.5 min time step or the sub-stepping time step? The latter would be more accurate.
 - a. **Response:** The cirrus model uses variable sub-stepping that is based on the 7.5 minutes of the model timestep but is calculated according to how S_i will evolve with the input updraft velocity such that changes in S_i equate to 1% for each cirrus model timestep. The cirrus timestep is

updated to 1 second after a threshold freezing process, like homogeneous nucleation, to better “capture the details after the nucleation event” (Münch, 2020) and then readjusted back to a longer timestep after the next cirrus timestep.

We added the detail of the dynamic sub-stepping to the text for clarity.

b. Change in the text at lines 206-207:

“The sub-stepping approach in the cirrus scheme is computed dynamically based on a 1.0 % rate of change of the ice saturation ratio between each sub-timestep.”

3. **Comment:** Lines 221-240: It would be useful to add a table summarizing the different ice nucleating properties, the sizes included, their ice saturation for nucleation and whether the AF treatment is used.

a. **Response:** This is a great idea. Please find an example of the proposed table below that we will include in the revised manuscript, with the last column indicating whether freezing occurs using active fraction (continuous) or through a threshold process, which is explained in more detail in the text.

Particle Type	Radius	Critical S_i	Freezing Mechanism	Freezing Method
Insoluble dust	0.05 – 0.5 μm	Temperature-dependent, but > 1.1	Deposition nucleation	Continuous
	> 0.5 μm	Temperature-dependent, but > 1.2		
Soluble dust	> 0.05 μm	1.3	Immersion freezing	Threshold
Aqueous Sulphate	All size modes from < 0.005 μm to > 0.5 μm	~1.4	Homogeneous nucleation	Threshold

4. **Comment:** Lines 253-255: Can you explain a bit more here? What is RH_i becomes 100% under a heterogeneous ice simulation?

a. **Response:** This refers to the default saturation adjustment approach, where any ice supersaturation used to form new ice particles is adjusted down to ice saturation ($RH_i = 100\%$) for the cloud fraction parameterisation and a cirrus cloud is assumed to fully cover a gridbox. With D19, this is no longer the case, as it allows for partial cirrus cloud fractions above ice saturation. We changed the example in the text to explain the difference between the two schemes more clearly. We also added text that provides more description in line with Figure 1 to make it clearer for readers.

b. **Changes in the text at lines 235-238, 243-247, and 247-249:**

“... This formulation works well for warm clouds, but as Kuebbeler et al. (2014) and Dietlicher et al. (2018, 2019) note, it breaks down for mixed-phase clouds ($T < 273$ K) that may or may not include ice, presenting a difficult choice between RH with respect to liquid (RH_l) or ice (RH_i) to determine cloud fraction. ...

... Dietlicher et al. (2019) updated the cloud fraction formulation for pure ice clouds to differ from liquid clouds by updating the RH conditions in which an ice cloud can partially cover a gridbox. In this new scheme (hereafter, D19) that we use in this study, ice saturation ($S_i = 1.0$) is set as the lower boundary condition for partial ice cloud fractions. The upper boundary condition for full gridbox coverage for ice clouds is set following the theory for homogeneous nucleation of solution droplets by Koop et al. (2000). ...

... As a contextual example, if ice were to form at 233 K in an environment with $S_i = 1.2$, then D19 would calculate an ice cloud fraction < 1.0 , whereas S89 would adjust the ice supersaturation down to ice saturation and would produce a cloud fraction of 1.0.”

5. **Comment:** Lines 265-267: This sentence needs more explanation. As it is now, I cannot understand what is being said.

a. **Response:** This refers to the scaling introduced to the available aerosol concentrations. The sentence was changed to make it clear that we apply scaling to the available aerosol concentration for each freezing mode to account for the aerosol particles that already nucleated ice crystals in previous time steps. This is necessary as no in-cloud aerosol tracers are available. The scaling was updated to account for only the fraction of each mode out of the total pre-existing ice. Previously the scaling was applied such that the total pre-existing ice concentration was removed from all modes, which resulted in an overestimation of the in-cloud aerosol concentration and an underestimation of the interstitial aerosol concentration.

b. **Change in the text at lines 253-257:**

“... The implementation of these tracers highlighted an error when accounting for the number of aerosols that previously nucleated ice. The aerosol concentration of each freezing mode of the cirrus scheme was scaled by the total amount of pre-existing ice. This approach overestimated the concentrations of in-cloud aerosols and underestimated the interstitial aerosol concentration. We updated the scaling of each mode aerosol concentration to account for the fraction of each mode out of the total pre-existing ice concentration. ...”

6. **Comment:** Line 279: Here you say you have a fractional ice cover scheme, but Lines 253-255 states that there is no fractional cover. When and where do you have fractional ice cover?

a. **Response:** Agreed. This is an inconsistency in the text, and it leaves out some important detail. The new D19 cloud fraction scheme allows for fractional cirrus coverage under ice formation conditions, as supersaturation is required. The default ECHAM S89 scheme would not allow this, where ice forming above ice saturation would be part of a cloud that would fully cover the gridbox. The manuscript was changed to clarify the description of the fractional ice-cloud cover

scheme related to your Comment 5 above. We also edited this line to remove ambiguity.

b. **Change in the text at line 272-273:**

“We performed cirrus seeding simulations using P3 with the cirrus scheme coupled to the new ice-cloud fraction approach (D19) described above.”

7. **Comment:** Lines 316-318: It appears to me that the model is too high from 190-205K by about the same factor as too high from 230-240. Please correct.

a. **Response:** We would argue that the disagreement between the model and the observations is not as consistent between 190-205K than it is between 230-240K. However, there is a noticeable difference and we amended the text to reflect that. In line with your next comment, we edited the text as well to note that the agreement above 240 K is better than the two temperature ranges quoted here but is slightly underpredicted.

b. **Change in the text at lines 309-310:**

“... Model-median ICNC values agree rather well with the observational median at temperatures between roughly 205K and 230K. ...”

8. **Comment:** Lines 319-321: Can you explain this statement better? Why do you think the finding is due to the dust immersion freezing rate? What aspect could cause this?

a. **Response:** In Figure 2a we see that between 230 and 240 K the model overpredicts ICNC, whereas above 240 K the model slightly underpredicts ICNC. We declare the cirrus regime at 238 K. Therefore, the disagreement in these two temperature ranges could be linked to a mixed-phase process. The Villanueva et al. (2021) study we cite looked into one such process in ECHAM, mixed-phase dust immersion freezing. In that study they compared the ECHAM-default rate-based parameterization for dust immersion freezing to a new active fraction (AF) approach. They note that using the new AF approach in combination with a higher dust-INP efficiency leads to better agreement with satellite observations, as the default rate-based approach underpredicts the amount of ice formation by dust immersion freezing in the mixed-phase regime. This leads to weak ice formation and a higher availability of cloud droplets from the mixed phase regime to be advected into the cirrus regime where they can freeze homogeneously, leading to a high ICNC just below the homogeneous temperature limit (238 K). We believe that the ICNC patterns we find in the model compared to the Krämer et al. (2020) observations reflect this issue. Model ICNC is slightly underpredicted above 240 K due to a too-slow mixed-phase dust immersion freezing rate that allows more cloud droplets to be advected into the cirrus regime and form excess ice at temperatures between 230 and 240 K.

b. **Change in the text at lines 313-320:**

“... The small disagreements in these two temperature ranges may be linked to the default parameterization for heterogeneous nucleation on mineral dust particles in mixed-phase clouds in ECHAM. The results by Villanueva et al. (2021) offer an explanation in this regard. In their study, they conducted several sensitivity tests with ECHAM-HAM using the default rate-based immersion freezing scheme by Lohmann and Diehl. (2006) and a newer AF approach based on dust particle surface area and active site density. They found better agreement with satellite-based observations using the AF approach in combination with higher dust particle freezing efficiency as compared to the default rate-based approach, and noted an under-prediction of mixed-phase ice with the latter that led to a higher abundance of cloud droplets being transported into the cirrus regime where they could undergo homogeneous nucleation. ...”

9. **Comment:** Lines 394-395: How can the change in ICNC (200 / L) be larger than the seeding number of 100?
- a. **Response:** The zonal anomalies we are presenting are the ICNC tracers we implemented into the model. The anomaly value can exceed the concentration of seeding particles for two reasons. Firstly, we use a simplified uniform seeding method in our model that does not include seeding-INP budgeting. This means that at every cirrus model timestep the same number of INPs is available and will activate if the S_i value is sufficient. This means we can achieve much higher ICNC values out of the cirrus scheme than the number of available seeding particles. Secondly, the ICNC variables are passed from the cirrus model to the microphysics scheme where they can be advected and/or undergo growth/shrink processes. With the anomaly value being so high, this also indicated that seeding at this concentration leads to more and smaller ice crystals that do not sediment out of the cirrus regime, but rather remain and increase the total ICNC. The combination of these two factors feeds into the overseeding response we find. We added a description related to the first point to the Experimental Setup section in the text to make this clearer for readers.
- b. **Change in the text at Line 278-281:**

“... For both model configurations (see Table 3) we implemented seeding particles as an additional heterogeneous freezing mode in the cirrus ice-nucleation scheme continuously at every timestep, following on from previous approaches (i.e. without accounting for those that already formed ice). Only gridboxes that are supersaturated with respect to ice (i.e. $S_i > 1.0$) are seeded. ...”

References

1. Münch, S., Development of a two-moment cloud scheme with prognostic cloud fraction and investigation of its influence on climate sensitivity in the global climate model ECHAM., *Doctoral Thesis*, <https://doi.org/10.3929/ethz-b-000454801>, 2020.
2. Villanueva, D., Neubauer, D., Gasparini, B., Ickes, L., and Tegen, I.: Constraining the Impact of Dust-Driven Droplet Freezing on Climate Using Cloud-Top-Phase Observations, *Geophysical Research Letters*, 48, <https://doi.org/https://doi.org/10.1029/2021GL092687>, 2021.

Cirrus cloud thinning using a more physically-based ice microphysics scheme in the ECHAM-HAM GCM (acp-2021-685)

Colin Tully, David Neubauer, Nadja Omanovic, and Ulrike Lohmann

David Mitchell Review Author Response

Dear David,

Firstly, we would like to thank you for taking the time to review our study and provide detailed feedback on a specific area for improvement. Regarding the orographic component of the vertical velocity by Joos et al. (2008, 2010), it was excluded from the first submission, as in initial tests we believed we were double counting the TKE and orographic components of the vertical velocity in grid cells where orography was active. This resulted in high ICNC values that did not provide us with confidence in our results. It turned out this was not the case and was merely down to a numerical issue, related to parallelization, when using the parameterization in ECHAM6.3 with the new P3 ice microphysics scheme (Morrison and Milbrandt, 2015; Dietlicher et al. 2018, 2019). After reworking the code to make it compatible with P3 we could easily include this vertical velocity component in our simulations. However, after re-running the Full_D19 reference simulation to verify this new approach, we found that including the orographic component is not needed when using the P3 microphysics scheme. In this response we provide our findings that support this claim, and lay out a solution that is implemented in the revised manuscript.

In the manuscript we validate our model with the in-situ measurements by Krämer et al. (2020). Figure 1, below, shows the model validation comparison between our original model that is presented in the manuscript (P3 Ref) and the revised model including the orographic velocity component (P3 Oro) for the reference Full_D19 simulation. It is clear that this extra component has an impact on the modelled ICNC values at lower temperatures ($T < 215$ K). The model no longer captures the higher frequency of low ICNC values at these temperatures. Instead, the model median is about two orders of magnitude higher than the observed median value. The high frequency ICNC of 1000 L^{-1} around 205 K is not present in the in-situ measurements. Furthermore, at higher temperatures, the model also does not capture frequent low ICNC values.

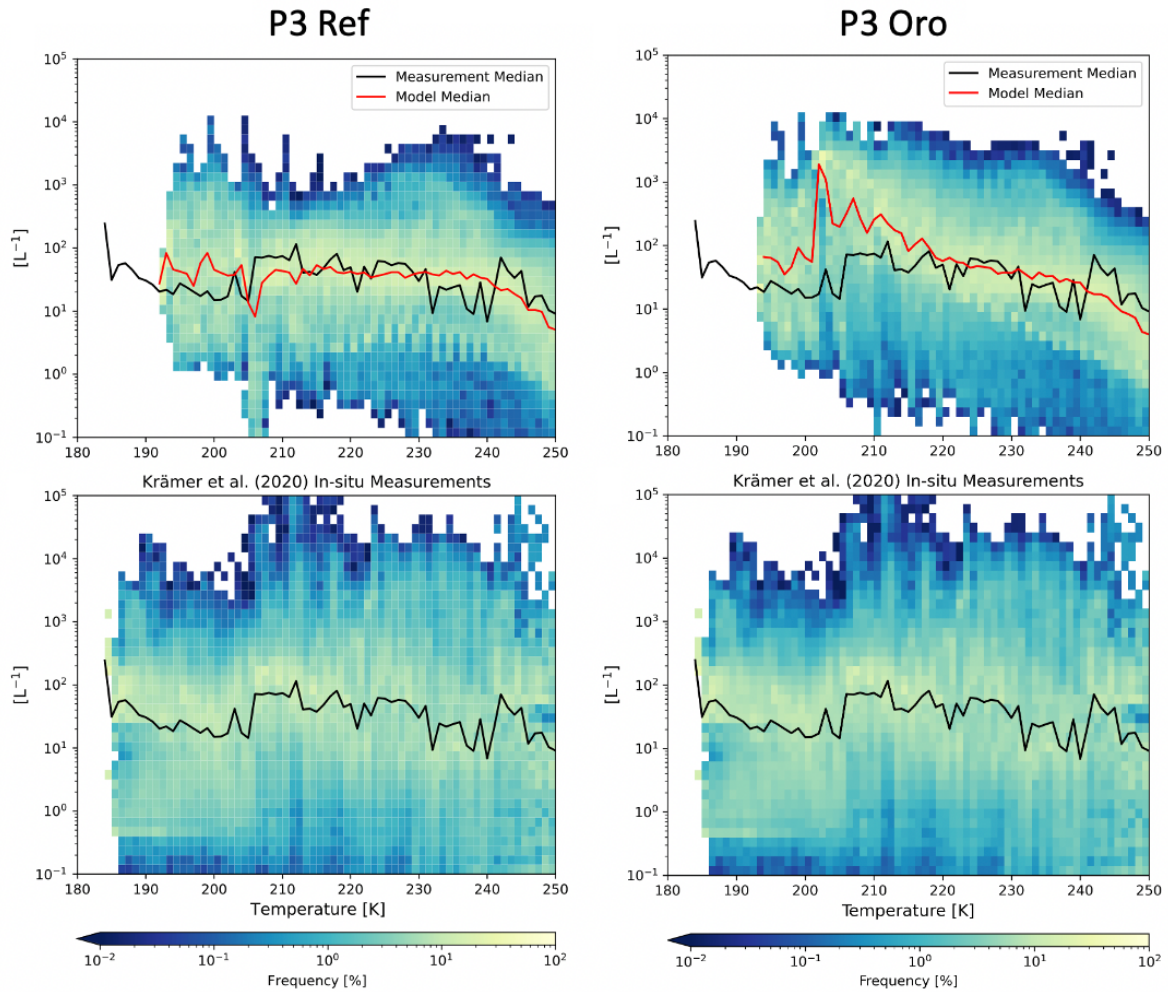


Figure 1: ICNC frequency diagrams for ice crystals with a diameter of at least $3 \mu\text{m}$ as a function of temperature between 180 K and 250 K binned like in Krämer et al. (2020) for every 1 K for P3 without the orographic velocity component (P3 Ref) and with the orographic velocity component (P3 Oro). The five-year global mean data from the model is plotted in the top row and the compilation of in-situ flight data from Krämer et al. (2020) is plotted in the bottom row. The red line in the upper plot represents the binned median ICNC value of the model data, and the black line in both plots is the same value for the observational data.

We examined this further by comparing our model to the DARDAR satellite remote-sensing ICNC dataset by Sourdeval et al. (2018) in Figure 2. Firstly, our model shows much wider ICNC variation than the DARDAR data for all temperature bins presented here. Muench and Lohmann (2020) note similar biases in their reference simulation associated with convective detrainment as well as the reduction of ice crystal sedimentation enhancement factors with their new cloud scheme. With the prognostic treatment of sedimentation with P3 (Dietlicher et al., 2018,2019), ice crystal removal is also slower and may contribute to high ICNC biases compared to DARDAR. Figure 3 shows the scatter of the modeled ICNC with and without the orographic component activated relative to the DARDAR ICNC dataset. We see that including the orographic component improves the correlation between the model and the satellite only between 223 and 233 K. For the colder temperature bins, activating the orographic velocity parameterization increases the root mean square error and worsens the correlation. However, the DARDAR data is not without its own biases that may not capture wider variability in the observed ICNC. Figure 4 from Krämer et

al. (2020) below shows the DARDAR retrieval frequency as well as ICNC percentiles for both the DARDAR dataset and the in-situ measurements. Firstly, it is noted that the majority of DARDAR measurements ($\sim 50\%$) are at temperatures > 225 K likely due to the overlapping occurrence of in-situ origin and liquid-origin cirrus clouds (Krämer et al., 2020; Wernli et al., 2016; Gasparini et al., 2018). However, what is important here is the variability of the ICNC values in the figure between the in-situ measurements (blue) and the DARDAR observations (red). Krämer et al. (2020) provide several reasons that explain the differences between the ICNC of these two observation platforms. Most notably is that DARDAR cannot detect the low ICNC associated with aged thin cirrus clouds at cold temperatures that were observed in the in-situ measurements. This is primarily due to insufficient sensitivity of the satellite instruments to these low ICNC values. A further bias originates from the assumptions made in the retrieval algorithm that is based on the parameterization by Delanoë et al. (2005) on particle size distribution (PSD) parameter constraints. As Sourdeval et al. (2018) note, this parameterization does not necessarily capture the multi-modality of the ice PSD observed in the in-situ measurements they compared in their study. This culminates in a potential overprediction of small ice crystals associated with high ICNC values at low temperatures that Krämer et al. (2020) explain is due to the transient nature of homogeneous nucleation and the complexities in observing this process in in-situ field campaigns. Finally, while our model shows more variability than the DARDAR data, likely as we can capture more regions of low ICNC at lower temperatures, it is within the range of the instantaneous in-situ measurement variability. In addition, by adding the orographic parameterization, high ICNC biases are enhanced due to the higher frequency of homogeneous nucleation, see below.

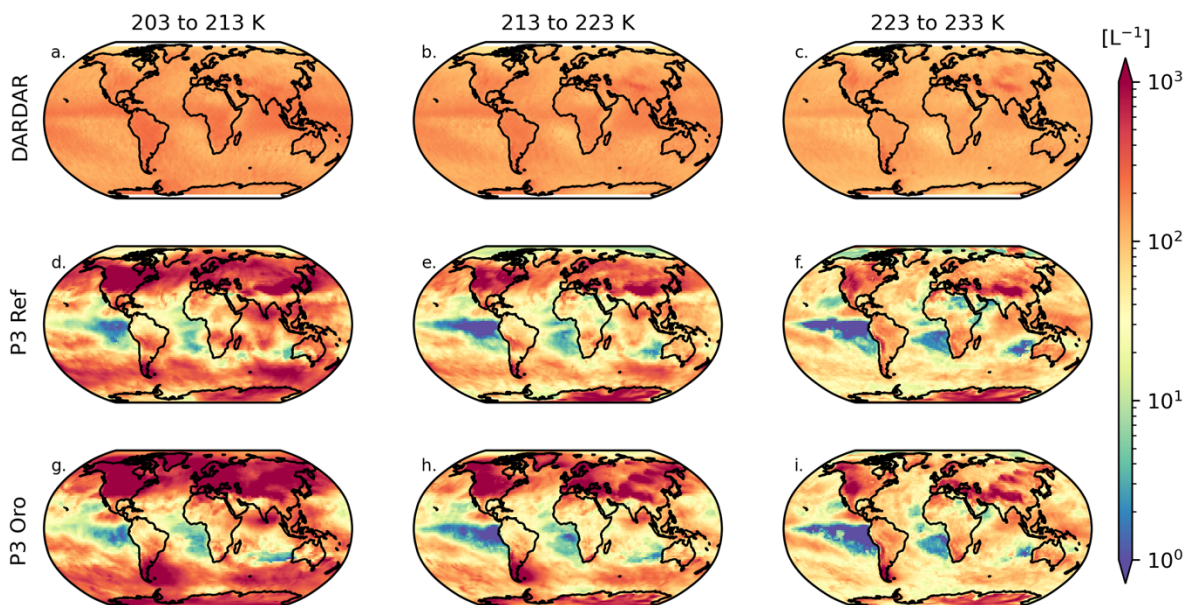


Figure 2: Spatial distribution of ICNC per DARDAR temperature bin. DARDAR data from Sourdeval et al. (2018) is plotted in a-c, 2010 annual mean model data without the orographic velocity component (P3 Ref) is plotted in d-f, and with the orographic velocity component in g-i.

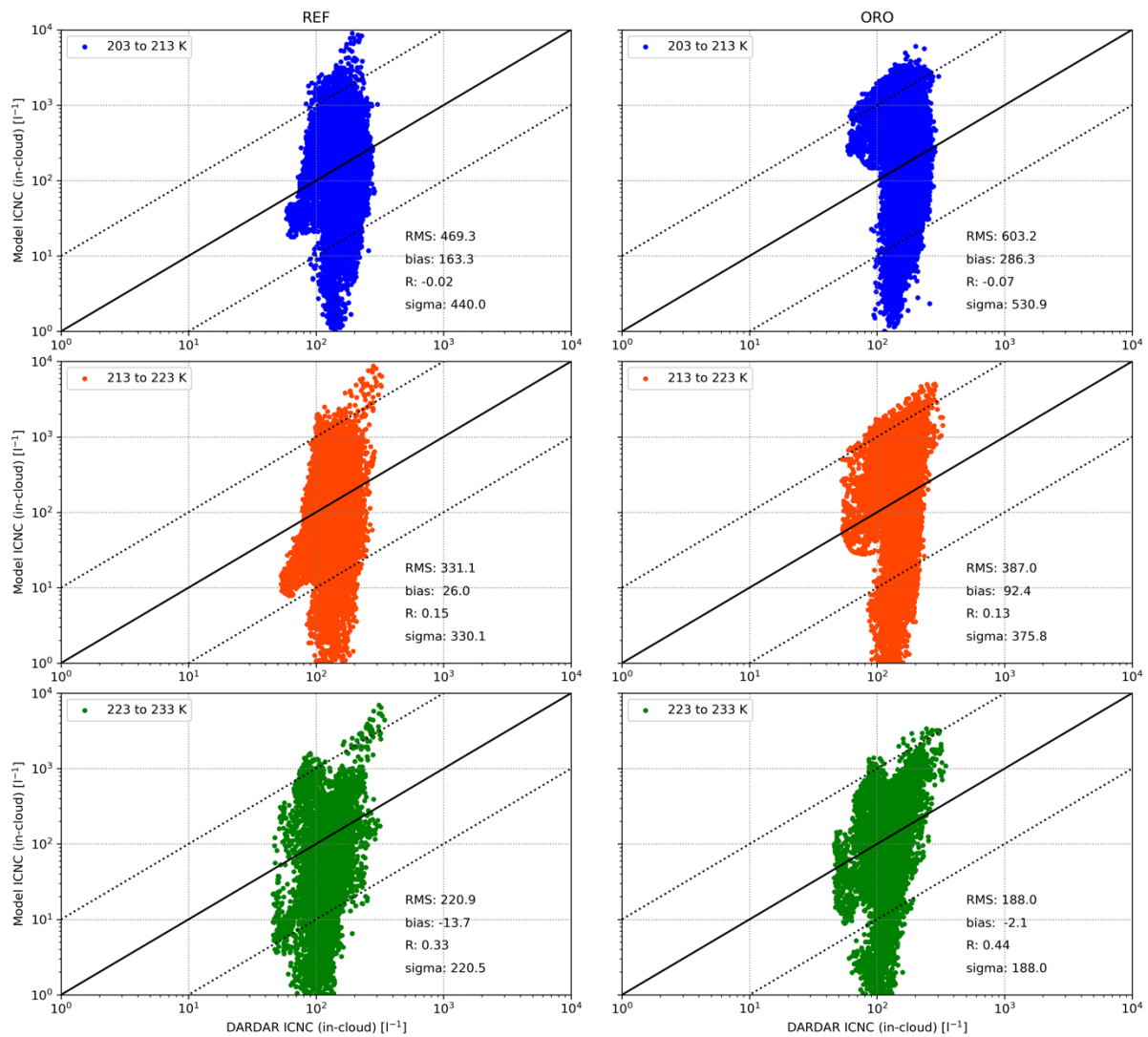


Figure 3: Adapted from Lohmann et al. (2020). Scatterplots of ICNC for the 2006-2016 annual mean DARDAR satellite remote-sensing dataset and the 2010 annual mean ECHAM-HAM ICNC for three DARDAR-defined temperature bins. The left column show the spread for the model without the orographic velocity component activated, and the right column the same but with the orographic component active. RMS is the root mean square error, R is the correlation coefficient, and sigma is the standard deviation of the difference between the modeled and satellite ICNC.

The key comparison is between P3 Ref (Figure 2d-f) and P3 Oro (Figure 2g-i). At the coldest temperatures between 203 and 213 K we find the highest mean ICNC values in our model for both P3 Ref and P3 Oro. In the former one can clearly see that mountainous regions around the Himalayas, the Andes, and the Rockies show local ICNC maxima. This is enhanced by adding the orographic velocity component in P3 Oro such that it weakens regional ICNC heterogeneity. In our P3 Ref simulation local ICNC maxima over mountainous regions become more apparent at higher temperatures, for example the elevated ICNC over Northern Chile and Southern Peru between 223 and 233 K (Figure 2f).

DARDAR $N_{\text{ice}} > 5 \mu\text{m}$ diameter

10 years climatology (2006 – 2016)

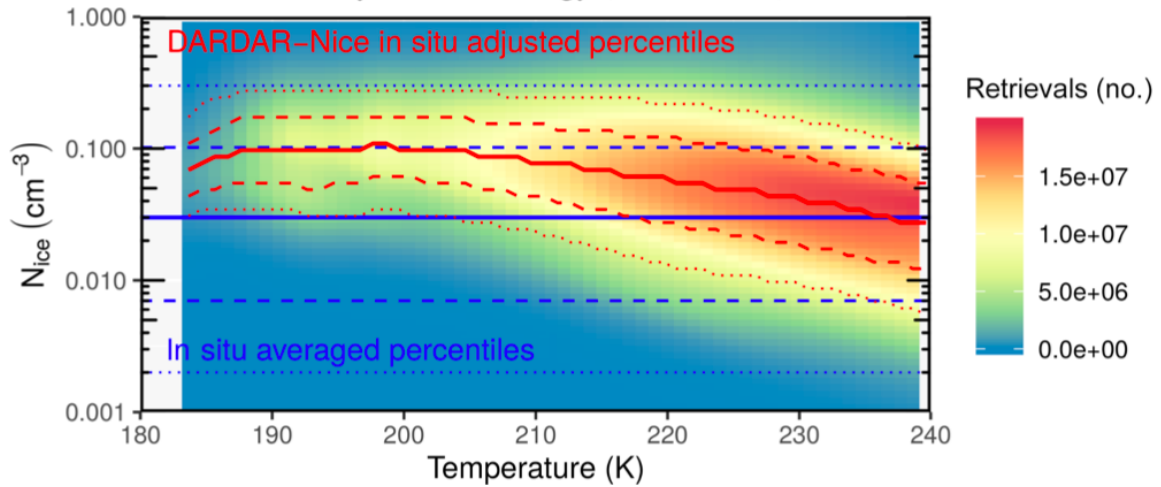


Figure 4: From Krämer et al. (2020). ICNC-temperature climatology. The colors in the background indicate the DARDAR retrieval frequency. The lines on the plot refer to the 10th and 90th (dotted), then 25th and 75th (dashed), and the 50th (solid) percentiles of DARDAR dataset (red) and the in-situ observations (blue).

Your main concern regarding our study as we understand it was that homogeneous nucleation within cirrus is underpredicted when excluding the orographic parameterization due to its strong dependence on vertical velocity. Figure 5 presents the ice number tracers at 200 hPa that were added to the model for this study. Like Figures 6 and 9 in the manuscript, these tracers represent the ice formed in-situ in the cirrus scheme that are then passed back to the microphysics scheme. Homogeneous nucleation forms the majority of in-situ cirrus ice in our model regardless of whether we include the orographic velocity component (Figure 5a and 5c). In fact, with this component activated homogeneous nucleation becomes more dominant, and like the DARDAR comparison above, some spatial heterogeneity is no longer evident. Heterogeneous nucleation also increases as critical ice saturation ratio values are reached more easily with the orographic component activated. Furthermore, Figure 6 is taken from Gasparini and Lohmann (2016) and shows the sources of cirrus ice using the default ECHAM microphysics scheme (2M) by Lohmann et al. (2007). Where heterogeneous nucleation was the dominant source of ice at 200 hPa for Gasparini and Lohmann (2016), that is not the case for our model with the P3 ice microphysics. Therefore, we argue that we do not underpredict homogeneous nucleation in in-situ cirrus in our model.

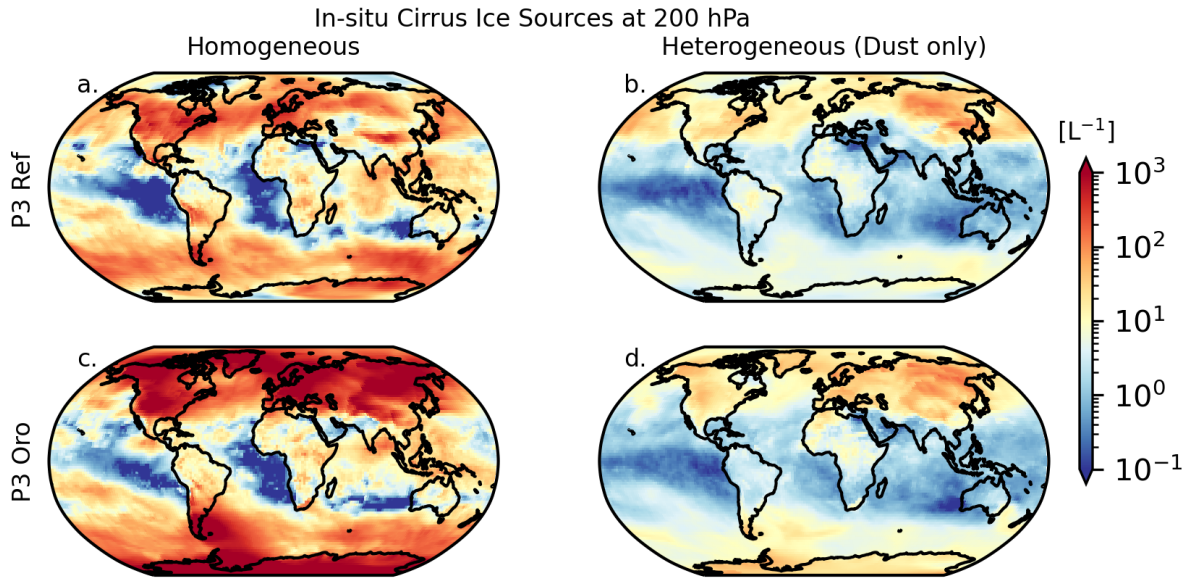


Figure 5: 2010 annual mean spatial distribution of in-situ ice number tracers on 200 hPa for the model without the orographic velocity component (a-b) and with the orographic velocity component (c-d).

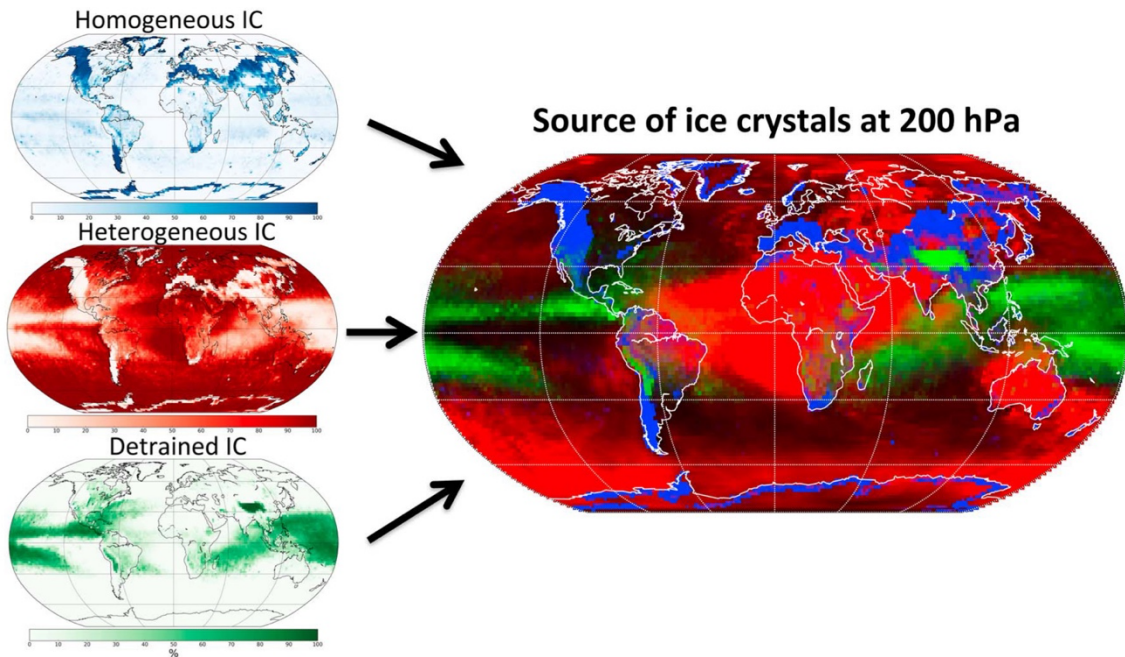


Figure 6: From Gasparini and Lohmann (2016), five year annual mean ice sources at 200 hPa for homogeneous nucleated ice, heterogeneously nucleated ice, and detrained ice crystals..

Based on the findings presented here, we conclude that the inclusion of the orographic velocity component is not needed with the P3 ice microphysics scheme. This highlights the fundamental difference between this newer microphysics scheme and the default ECHAM scheme (2M) by Lohmann et al. (2007) that was used in previous studies from our group (Gasparini and Lohmann, 2016; Gasparini et al., 2017). P3 utilizes prognostic sedimentation of ice hydrometeors by simulating the ice population using a single category, whereas the 2M scheme separates ice into two classes, in-cloud and precipitating. In order to maintain cloud-ice values and cloud radiative properties within the range of observations with the 2M scheme, ice

removal was sped up by enhancing ice crystal aggregation to form snow (Neubauer et al., 2019). This is no longer necessary with P3 as the size-class separation is no longer included in the model, and the updated cloud fraction scheme allows for fractional cirrus cloud cover above ice saturation. The result is much slower ice removal via sedimentation. We can clearly see the effects of this behavior in the plots presented here. Large ICNC values at the coldest temperatures (Figure 2d), originating predominantly from homogeneous nucleation (Figure 5a), are already achieved in our model. With the prognostic sedimentation in our model, these small ice crystals remain in the atmosphere for an extended period. The effect of the orographic velocity component is only to enhance homogeneous nucleation and form more ice that remains in the atmosphere for an even longer time period. We argue that while the orographic component was vital for ensuring homogeneous nucleation was not underpredicted when using the 2M scheme, it is no longer needed with the P3 scheme.

In conclusion, we excluded the orographic velocity component from our study based on our findings. However, as this is the first time the P3 ice microphysics scheme was validated with and without this component, we added an Appendix to the revised manuscript directly after the conclusions with the figures and explanations presented here.

Sincerely,
Colin Tully (on behalf of all co-authors)

References

- Delanoë, J., Protat, A., Testud, J., Bouniol, D., Heymsfield, A. J., Bansemmer, A., Brown, P. R. A., and Forbes, R. M.: Statistical properties of the normalized ice particle size distribution, *Journal of Geophysical Research: Atmospheres*, 110, <https://doi.org/10.1029/2004JD005405>, <https://agupubs.onlinelibrary.wiley.com/doi/abs/10.1029/2004JD005405>, 2005.
- Dietlicher, R., Neubauer, D., and Lohmann, U.: Prognostic parameterization of cloud ice with a single category in the aerosol-climate model ECHAM(v6.3.0)-HAM(v2.3), *Geoscientific Model Development*, 11, 1557–1576, <https://doi.org/10.5194/gmd-11-1557-2018>, <https://gmd.copernicus.org/articles/11/1557/2018/>, 2018.
- Dietlicher, R., Neubauer, D., and Lohmann, U.: Elucidating ice formation pathways in the aerosol–climate model ECHAM6-HAM2, *Atmospheric Chemistry and Physics*, 19, 9061–9080, <https://doi.org/10.5194/acp-19-9061-2019>, <https://www.atmos-chem-phys.net/19/9061/2019/>, 2019.
- Gasparini, B. and Lohmann, U.: Why cirrus cloud seeding cannot substantially cool the planet, *Journal of Geophysical Research: Atmospheres*, 121, 4877–4893, <https://doi.org/10.1002/2015JD024666>, <https://agupubs.onlinelibrary.wiley.com/doi/abs/10.1002/2015JD024666>, 2016.
- Gasparini, B., Münch, S., Poncet, L., Feldmann, M., and Lohmann, U.: Is increasing ice crystal sedimentation velocity in geoengineering simulations a good proxy for cirrus cloud seeding?, *Atmospheric Chemistry and Physics*, 17, 4871–4885, <https://doi.org/10.5194/acp-17-4871-2017>, <https://acp.copernicus.org/articles/17/4871/2017/>, 2017.
- Gasparini, B., Meyer, A., Neubauer, D., Münch, S., and Lohmann, U.: Cirrus Cloud Properties as Seen by the CALIPSO Satellite and ECHAM-HAM Global Climate Model, *Journal of Climate*, 31, 1983–2003,

<https://doi.org/10.1175/JCLI-D-16-0608.1>, <https://doi.org/10.8351175/JCLI-D-16-0608.1>, 2018.

- Joos, H., Spichtinger, P., and Lohmann, U.: Orographic cirrus in the global climate model ECHAM5, *Journal of Geophysical Research*, 113, <https://doi.org/10.1029/2007JD009605>, <https://agupubs.onlinelibrary.wiley.com/doi/abs/10.1029/2007JD009605>, 2008.
- Joos, H., Spichtinger, P., and Lohmann, U.: Influence of a future climate on the microphysical and optical properties of orographic cirrus clouds in ECHAM5, *Journal of Geophysical Research: Atmospheres*, 115, <https://doi.org/https://doi.org/10.1029/2010JD013824>, <https://agupubs.onlinelibrary.wiley.com/doi/abs/10.1029/2010JD013824>, 2010.
- Krämer, M., Rolf, C., Spelten, N., Afchine, A., Fahey, D., Jensen, E., Khaykin, S., Kuhn, T., Lawson, P., Lykov, A., Pan, L. L., Riese, M., Rollins, A., Stroh, F., Thornberry, T., Wolf, V., Woods, S., Spichtinger, P., Quaas, J., and Sourdeval, O.: A microphysics guide to cirrus – Part 2: Climatologies of clouds and humidity from observations, *Atmospheric Chemistry and Physics*, 20, 12 569–12 608, <https://doi.org/10.5194/acp-20-12569-2020>, <https://acp.copernicus.org/articles/20/12569/2020/>, 2020.
- Lohmann, U., Stier, P., Hoose, C., Ferrachat, S., Kloster, S., Roeckner, E., and Zhang, J.: Cloud microphysics and aerosol indirect effects in the global climate model ECHAM5-HAM, *Atmospheric Chemistry and Physics*, 7, 3425–3446, <https://doi.org/10.5194/acp-7-3425-2007>, <https://www.atmos-chem-phys.net/7/3425/2007/>, 2007.
- Lohmann, U., Friebel, F., Kanji, Z., Mahrt, F., Mensah, A., and Neubauer, D.: Future warming exacerbated by aged-soot effect on cloud formation, *Nature Geoscience*, 13, 674–680, <https://doi.org/10.1038/s41561-020-0631-0>, <https://doi.org/10.1038/s41561-020-0631-0>, 2020.
- Morrison, H. and Milbrandt, J. A.: Parameterization of Cloud Microphysics Based on the Prediction of Bulk Ice Particle Properties. Part I: Scheme Description and Idealized Tests, *Journal of the Atmospheric Sciences*, 72, 287–311, <https://doi.org/10.1175/JAS-D-14-0065.1>, <https://doi.org/10.1175/JAS-D-14-0065.1>, 2015.
- Neubauer, D., Ferrachat, S., Siegenthaler-Le Drian, C., Stier, P., Partridge, D. G., Tegen, I., Bey, I., Stanelle, T., Kokkola, H., and Lohmann, U.: The global aerosol–climate model ECHAM6.3–HAM2.3 – Part 2: Cloud evaluation, aerosol radiative forcing, and climate sensitivity, *Geoscientific Model Development*, 12, 3609–3639, <https://doi.org/10.5194/gmd-12-3609-2019>, <https://gmd.copernicus.org/articles/12/3609/2019/>, 2019.
- Sourdeval, O., Gryspeerdt, E., Krämer, M., Goren, T., Delanöe, J., Afchine, A., Hemmer, F., and Quaas, J.: Ice crystal number concentration estimates from lidar–radar satellite remote sensing -- Part 1: Method and evaluation, *Atmospheric Chemistry and Physics*, 18, 14327–14350, <https://doi.org/10.5194/acp-18-14327-2018>, <https://acp.copernicus.org/articles/18/14327/2018/>, 2018.
- Wernli, H., Boettcher, M., Joos, H., Miltenberger, A.K., and Spichtinger, P.: A trajectory-based classification of ERA-Interim ice clouds in the region of the North Atlantic storm track, *Geophysical Research Letters*, 43, 6657–6664, <https://doi.org/10.1002/2016GL068922>, <https://agupubs.onlinelibrary.wiley.com/doi/abs/10.1002/2016GL068922>, 2016.

Cirrus cloud thinning using a more physically-based ice microphysics scheme in the ECHAM-HAM GCM (acp-2021-685)

Colin Tully, David Neubauer, Nadja Omanovic, and Ulrike Lohmann

Referee #4 Author Response

Thank you for taking the time to review our manuscript and providing useful comments on improving this study. We have quoted each of your comments below with our response.

10. **Comment:** It might be helpful to take a step back and better validate both the shortwave (SW) and longwave (LW) cloud radiative effect (CRE) in the model. After model tuning, it was mentioned on lines 275-277 that the net CRE was too negative and that the 5-year global LW CRE is weaker than the observed range. What is this “structural issue within the model” on line 276 referring to and why does it cause a presumably more negative SW CRE? What is the cause for the CRE biases? Is it due to differences in cloud fraction, cloud height or cloud optical thickness?

- a. While SW as well as LW CRE global mean values are within observational ranges the net CRE is not. This was recognized in different configurations of ECHAM-HAM (e.g. Dietlicher et al., 2019; Neubauer et al., 2019). Furthermore, this holds for many different parameter configurations (not shown) and therefore points towards a possible structural error (e.g. Johnson et al., 2020). Neubauer et al. (2019) report an underestimation of stratocumulus clouds but the exact nature of the possible structural problem is not known. Therefore, we amended the text between **Lines 268-270** to read:

“We also note a too negative net CRE after tuning. Dietlicher et al. (2019) state this points to a possible structural problem within the model, which relates to the coarse vertical resolution that results in the under-prediction of low-level clouds (Pelucchi et al., 2021).”

- b. In response to your question on what could cause this structural issue, Dietlicher et al. (2019) report an improved vertical structure and high-level cloud fraction in ECHAM-HAM with the P3 scheme but an underestimation of mid- and low-level cloud fractions. They further report an underestimation of cloud ice compared to satellite observations, but part of this underestimation is due to the satellite observations, including convective precipitation, which was not included in the ECHAM-HAM-P3 total ice water content. This underestimation is related to a known problem in ECHAM, involving the coarse vertical resolution employed in the model. A recent study by Pelucchi et al. (2021) reported that low-level stratocumulus clouds extent is underpredicted due to poor representation of the vertical relative humidity profile, and low-level cloud occurrence frequency.

- c. A few of your comments focused on SW and LW CRE. Therefore, we decided to collate our explanations related to the changes in the manuscript here for ease. This relates to Comments #1, 4d, 5a, and 7a. Tables 2 and 3 (now Tables 4 and 5 in the revised manuscript) were reconfigured to reflect the SW and LW CREs as well as the 95% confidence interval, see the example layout below. We decided to keep Figure 3 as is to avoid a plot that is too cumbersome. **Lines 344-360**, and **474-489** were reworked to reflect the changes to the Tables.

Reconfigured Tables 2 and 3 (now Tables 4 and 5, with values provided in revised manuscript)

Seeding Concentration [L ⁻¹]		0.1	1	10	100
D19	Net TOA				
	Net CRE				
	SWCRE				
	LWCRE				
S89	Net TOA				
	Net CRE				
	SWCRE				
	LWCRE				

11. **Comment:** Although P3 is a more physically-based ice microphysics scheme, does it result in ice removal processes that are more *realistic*? Please include a discussion in the context of snowfall.

- a. We partially agree with this comment. The vertical velocity of hydrometeors is no longer tuned using the P3 scheme as it is in the default microphysics scheme (Lohmann et al., 2007), and is instead based on particle mass-to-size relationships. Therefore, in the context of sedimentation velocity, we can state that P3 uses a more realistic approach. However, we cannot state whether the P3 scheme is more realistic in the context of other microphysical processes (e.g. accretion, aggregation, etc.). Therefore, we can merely state that the P3 scheme uses a more physically based representation of ice microphysics, which leads to much larger radiative responses due to slower ice removal processes as compared to the default EHCAM microphysics scheme (Lohmann et al., 2007).
- b. **Changes in the text at lines 16-17 in the abstract, and Point #2 under in conclusions:**

“This effect is amplified by longer ice residence times in clouds due to the slower removal of ice via sedimentation in the P3 scheme.”

“The prognostic treatment of sedimentation in the P3 microphysics scheme, leading to slower and more physically-based ice removal, is likely the reason why we find such large seeding responses compared to the study by Gasparini and Lohmann (2016), using the default ECHAM 2M scheme. Our model produces smaller and more numerous ice particles

that amplify the already longer ice residence times within clouds to induce a strong positive TOA forcing.”

12. **Comment:** The tuning in the model appears to be quite arbitrary. To reduce the overseeding effect in the model, the authors increased $S_{i,seed}$ to 1.35. Why was this particular value chosen, e.g. why not 1.4 or 1.45?

Response to critical S_i value: We chose to increase the critical seeding ice saturation ratio (S_i) from 1.05 to 1.35 for two reasons. First, at this value we avoid impacting heterogeneous nucleation on mineral dust as much as possible, which can occur via immersion freezing at a minimum S_i of 1.3; dust deposition freezing can initiate at lower S_i values. Second, we did not want to make the seeding S_i value higher so that seeding particles remain competitive with homogeneous nucleation in our cirrus model, which can occur at a minimum S_i value of roughly 1.4. We believe this is justified as this is the first time in a CCT study using a GCM that the sensitivity to the critical S_i value was tested. As our results show that this in fact appears to be an important factor determining CCT efficacy, we argue it is justified as a new finding relative to previous CCT studies that could be used to inform further work into this geoengineering proposal.

13. **Comment:** I disagree with the statement that the model “agrees remarkably well with the Kramer et al. (2020) measurements for in-situ formed cirrus” (lines 340-341). The discussion comparing the modelled and measured ICNC appears to be only based on the median values. It appears that there is a large discrepancy in the 215 K to 250 K range for relatively low ICNC (bottom right of plot) which is unexplained. Also, did the Karcher et al. in situ measurements account for the ice crystal shattering effects on probes? Lines 452-454 also seem inaccurate because a small cooling effect is not seen for all seeding concentrations other than S89 Seed100 in Table 3--- it is also small and positive for 5 other values too.

- a. **Response:** This appears to be three separate comments. Therefore, we have divided them into the following sub-points:
- b. **Response to first statement on missing explanation for low ICNC values:** We agree that this explanation should be included in the manuscript. The model agrees well for median values but misses lower ICNC values because we plot annual mean data, whereas the in-situ measurements are instantaneous. **Changes in the text at lines 338-342:**

“The model also does not capture the wide variability of ICNC values as seen in the in-situ measurements, as we compare five-year annual mean model data to instantaneous values recorded during various aircraft campaigns. However, for the purposes of our CCT analysis we find that the model median ICNC as a function of temperature agrees well with the Krämer et al. (2020) measurements for in-situ formed cirrus.”

- c. **Response to ice crystal shattering:** Yes, Krämer et al. (2020) considered ice crystal shattering in their results and aimed to minimize its effect on older datasets where possible. See their Appendix A2.4.
- d. **Response to second statement on cooling effect:** We disagree with this comment as what you are referring to is the net CRE anomalies in Table 3 (now Table 4 in the revised manuscript). What we cover in Lines 452-454 is the net TOA anomalies, of which all the mean values show a slight cooling effect except S89 Seed100. This is also consistent with Table 3. We agree that there should be some discussion of the net CRE anomalies in line with Figure 3 and Table 3 in this paragraph to make it clearer. For ease, please see the response under Comment #1.

14. **Comment:** Given the competing effects of CCT on both the SW and LW CRE, I would recommend including the breakdown of these effects (as opposed to only the net CRE) in Table 2, Table 3 and Figure 3.

- a. **Response:** We agree with this assessment. The breakdown of the SW and LW CREs is useful in order to understand the impact seeding has on cloud properties. In order to avoid a cumbersome figure, we refrained from adding it to Figure 3, but instead expanded Tables 2 and 3 (now Tables 4 and 5 in the revised manuscript) to show this effect. For ease, please see the response under Comment #1.

15. **Comment:** Figure 5: Please carefully explain the unexpected result of the heterogeneous change in ICNC.

- a. **Response:** We agree that this is not covered in enough detail. This was amended in the text to include a better description of this heterogeneous signal, which also links to the Stratospheric Impacts section further down in the results.
- b. **Changes in the text at lines 400-403 and 422-428:**

“The ICNC anomalies are much clearer and certain for the extreme case, Seed100, than for the Seed1 anomalies (Figure 5c-d). Positive ICNC anomalies exceeding 200 L⁻¹ are shown at all latitudes throughout the troposphere, and into the lower stratosphere at higher latitudes. The anomaly heterogeneity around the tropics is likely due to the proficiency of seeding particles to nucleate ice and hamper homogeneous nucleation in convective outflow regions around the tropopause. ...”

“... The shift of homogeneous nucleation to lower pressure levels (Figure 6a-b), is likely due to increased LW cloud-top cooling from thicker cirrus cloud following seeding (Possner et al., 2017). This also impacts heterogeneous nucleation on mineral dust particles in the lower stratosphere. As this latter process is not sufficient at consuming water vapor, homogeneous nucleation proceeds to form additional ice crystals. This cloud top cooling effect likely also explains the heterogeneity of the total ICNC anomaly around the tropical tropopause (Figure 5). As there is a clear separation between the troposphere and the stratosphere, these phenomena point to a complex impact on the stratospheric circulation, which we discuss in Section 3.4.”

16. **Comment:** Does the intended side effect of CCT on mixed-phase clouds dominate the intended main effect on CCT? The impact on mixed-phase clouds in Figs 7 and 11 seem quite large. Please discuss. I would also recommend adding this result to the Abstract as well.

- a. **Response:** This was discussed in lines 417-427. In the revised manuscript, this is now discussed between lines 429-442, and 560-576. For $S_i = 1.05$ with a seeding particle concentration of 100 L^{-1} we find an impact on lower-lying MPCs through less efficient MP processes that enhances the SWCRE. However, this is outweighed now by the overseeding effect on LWCRE from more numerous and smaller ice crystals in cirrus clouds. For ease, please see the response under Comment #1. In terms of the abstract, we included this with the line: “*due mostly to rapid cloud adjustments*”. However, as this is ambiguous, we amended the text in the abstract at **Line 24-27:**

“Our results also show feedbacks on lower-lying mixed-phase and liquid clouds through the reduction of ice crystal sedimentation that reduces cloud droplet depletion and results in stronger cloud albedo effects. However, this is outweighed by stronger longwave trapping from cirrus clouds with more numerous and small ice crystals.”

17. **Comment:** What is the reason for the isolated southern hemisphere cooling effect in the summer due to seeding with $S_{i,seed} = 1.35$ in Fig. 10?

- a. **Response:** We are unsure whether this refers to the summer quoted on the figure (second row) or southern hemisphere summer (top row). For the former, the isolated areas of SH cooling were due to weaker LWCRE as there is no SWCRE during this season. This points to wintertime seeding having the desired effect in these small regions. If you are referring to the latter (SH summer), which is what we have assumed for the revised text, then small regions of cooling are related to the feedback we find related to MPCs. We agree this is not appropriately covered in the manuscript and have revised the text between lines 546 and 528 to cover more of what we find in Figure 10. Here we quote the text referring to our new results.
- b. **Additional text between Lines 553-565:**

We also find smaller regions of cooling with net negative TOA responses for Seed1 during NH winter in the SH (summer) around 45°S , and between the Equator and 30°S (Figure 10a). The net TOA response is driven mainly by negative SW anomalies, indicating either a shift in cirrus formation pathway or an impact on lower-lying mixed phase clouds.

During NH summer the net TOA response is smaller overall than during NH winter. For the Seed1_1.35 zonal mean anomaly we find only small regions of cooling in the NH and in the SH polar regions. However, the uncertainty is wide enough in this case that we cannot determine exact radiative impact in these regions. The small amount cooling shown towards high latitudes in the SH is driven by LW reductions due to a lack of SW radiation in this

region during the period, but like the net TOA anomaly is highly uncertain. The few regions of cooling we find in the NH are driven by SW anomalies, highlighting a potential feedback on cirrus cloud formation or on mixed-phase clouds, but are compensated by positive LW anomalies. This is especially noticeable in the northern hemisphere tropics around the location of the Intertropical Convergence Zone (ITCZ). Thicker in-situ cirrus clouds to some extent reflect more SW (Krämer et al., 2020), similar to the Twomey effect for lower-lying liquid or MPCs. However, they also induce a strong compensating LW effect as a result of seeding.

Minor:

1. **Comment:** Please include letter labels for every panel of all multi-panel plots.
 - a. **Response:** This is a good point. After double-checking, you are referring to Figures 4, 6, and 9. We amended our plotting scripts for these figures to include lettering for multiple plots and have adjusted the text where necessary to reference a specific plot.
2. **Comment:** Line 302: “cannot not” double negative. I think you mean “cannot”?
 - a. **Response:** Thank you for pointing that out. We do mean “cannot”. The manuscript was edited to delete the double negative.

References

3. Dietlicher, R., Neubauer, D., and Lohmann, U.: Elucidating ice formation pathways in the aerosol–climate model ECHAM6-HAM2, *Atmospheric Chemistry and Physics*, 19, 9061–9080, <https://doi.org/10.5194/acp-19-9061-2019>, 2019.
4. Johnson, J. S., Regayre, L. A., Yoshioka, M., Pringle, K. J., Turnock, S. T., Browse, J., Sexton, D. M. H., Rostron, J. W., Schutgens, N. A. J., Partridge, D. G., Liu, D., Allan, J. D., Coe, H., Ding, A., Cohen, D. D., Atanacio, A., Vakkari, V., Asmi, E., and Carslaw, K. S.: Robust observational constraint of uncertain aerosol processes and emissions in a climate model and the effect on aerosol radiative forcing, *Atmospheric Chemistry and Physics*, 20, 9491–9524, <https://doi.org/10.5194/acp-20-9491-2020>, 2020.
5. Krämer, M., Rolf, C., Luebke, A., Afchine, A., Spelten, N., Costa, A., Meyer, J., Zöger, M., Smith, J., Herman, R. L., Buchholz, B., Ebert, V., Baumgardner, D., Borrmann, S., Klingebiel, M., and Avallone, L.: A microphysics guide to cirrus clouds – Part 1: Cirrus types, *Atmospheric Chemistry and Physics*, 16, 3463–3483, <https://doi.org/10.5194/acp-16-3463-2016>, 2016.
6. Lohmann, U., Stier, P., Hoose, C., Ferrachat, S., Kloster, S., Roeckner, E., and Zhang, J.: Cloud microphysics and aerosol indirect effects in the global climate model ECHAM5-HAM, *Atmospheric Chemistry and Physics*, 7, 3425–3446, <https://doi.org/10.5194/acp-7-3425-2007>, 2007.
7. Mauritsen, T., Stevens, B., Roeckner, E., Crueger, T., Esch, M., Giorgetta, M., Haak, H., Jungclaus, J., Klocke, D., Matei, D., Mikolajewicz, U., Notz, D., Pincus, R., Schmidt, H., and Tomassini, L.: Tuning the climate of a global model, *Journal of Advances in Modeling Earth Systems*, 4, <https://doi.org/10.1029/2012MS000154>, 2012.

8. Neubauer, D., Ferrachat, S., Siegenthaler-Le Drian, C., Stier, P., Partridge, D. G., Tegen, I., Bey, I., Stanelle, T., Kokkola, H., and Lohmann, U.: The global aerosol–climate model ECHAM6.3–HAM2.3 – Part 2: Cloud evaluation, aerosol radiative forcing, and climate sensitivity, *Geoscientific Model Development*, 12, 3609–3639, <https://doi.org/10.5194/gmd-12-3609-2019>, 2019.
9. Pelucchi, P., Neubauer, D., and Lohmann, U.: Vertical grid refinement for stratocumulus clouds in the radiation scheme of the global climate model ECHAM6.3-HAM2.3-P3, *Geoscientific Model Development*, 14, 5413-5434, <https://doi.org/10.5194/gmd-14-5413-2021>, 2021.